Załącznik nr 3

SCIENTIFIC CURRICULUM VITAE
(Autoreferat)

Seismic receiver function – techniques of analysis of the lithospheric and mantle trasition zone's structures

dr Monika Wilde-Piórko

Lithospheric Physics Department, Institute of Geophysics,

Faculty of Physics, University of Warsaw

CONTENTS

1. First and last name

Monika Wilde-Piórko

2. Diplomas and scientific degrees, including date of award and name, location of awarding institution, and title of PhD dissertation

1997 — Professional title of MSc obtained in scope of physics, specialty: physics of lithosphere; Faculty of Physics, University of Warsaw; title of MSc dissertation: "Crustal seismic structure based on the receiver function of Suwałki station";
2002 — PhD degree in scope of physics; awarded by the Scientific Council of Faculty of Physics, University of Warsaw; title of the PhD thesis: "Modelling of seismic structure of the crust and upper mantle from receiver function".

3. Information on previous and current employment in research institutions

1997–2002 – PhD studies, Faculty of Physics, University of Warsaw;
from **2002** — assistant professor (adjunct), Institute of Geophysics, Faculty of Physics, University of Warsaw;
including:
maternity leave: 09.12.2003–29.03.2004 and 29.12.2006–17.05.2007;
parental leave: 08.06.2004–30.09.2004 and 06.08.2007–14.09.2007;
medical leave: 12.10.2006–28.12.2006.

4. Scientific achievements as per art. 16, p. 2 law dated on 14 March 2003 on the scientific degrees and on the scientific titles and on the degrees and the titles in scope of arts (Polish: Dz. U. 2016 r. poz. 882 ze zm. w Dz. U. z 2016 r. poz. 1311)

4.1. Title of the scientific achievement

Seismic receiver function – techniques of analysis of the lithospheric and mantle trasition zone's structures

4.2. List of publications constituting scientific achievement

H1. **Wilde-Piórko, M.**, Saul, J. and Grad, M., **2005**. Differences in the crustal and uppermost mantle structure of the Bohemian Massif from teleseismic receiver functions,

Studia Geophysica et Geodaetica, 49, 85–107, DOI: 10.1007/s11200-005-1627-3.

H2. Wilde-Piórko, M., Świeczak, M., Grad, M. and Majdański, M., **2010**. Integrated seismic model of the crust and upper mantle of the Trans-European Suture Zone between the Precambrian craton and Phanerozoic terranes in the Central Europe, *Tectonophysics*, 481, 108–115, DOI: 10.1016/j.tecto.2009.05.002.

H3. Trojanowski, J. and **Wilde-Piórko, M., 2012**. S-Velocity Structure Beneath the Bohemian Massif from Monte Carlo Inversion of Seismic Receiver Function, *Acta Geophysica*, 60 (1), 76–91, DOI: 10.2478/s11600-011-0047-8.

H4. Wilde-Piórko, M., 2015. Crustal and upper mantle seismic structure of the Svalbard Archipelago from the receiver function analysis, *Polish Polar Research*, 36 (2), 89–107, DOI: 10.1515/popore-2015-0009.

H5. Wilde-Piórko, M., Grycuk, M., Polkowski, M. and Grad, M., **2017**. On the rotation of teleseismic seismograms based on the receiver function technique, *Journal of Seismology*, DOI: 10.1007/s10950-017-9640-x.

4.3. Discussion of the scientific goal and presentation of the obtained results, including discussion of the possible applications

Scientific goal of achievement. The scientific goal of achievement was the development of new techniques of rotation and selection of the receiver function which can be used for an automatic calculation of receiver function for a large data set and in a determination of the seismic structure of different tectonic units to the depth of about 900 km. In recent years there has been rapid development of research equipment used in seismology, and thus a huge increase in the amount of measured data are observed. Therefore, there is necessary to develop new methods of analysis of seismic data to cope with these challenges and provide information about the structure of upper layers of Earth in the local and regional scale.

Introduction. For the first time receiver function has been used to analysis the seismic data at the end of the seventies of the twentieth century (Langston, 1977a; Vinnik, 1977). A seismic station can measure a montion of the Earth's surface caused by seismic waves generated during earthquakes. A trace recorded by the seismic station are called a seismogram and for teleseismic earthquakes from epicentral distances 30°–98° is a convolution of three functions: S(t) – a characteristic of the source of the earthquake, I(t) – a transfer function of the receiver and E(t) – an impulse response of the structure for incoming waves travelling from the source to the receiver. In the case of recording of the direct longitudinal wave (P – the first recorded wave) the function describing the seismic source is not

directionally dependent. A seismogram recorded by the seismic station can be described by the following formulas:

$$D_Z(t) = I(t) * S(t) * E_Z(t) \,, \tag{1}$$

$$D_N(t) = I(t) * S(t) * E_N(t) \,, \tag{2}$$

$$D_E(t) = I(t) * S(t) * E_E(t) \,, \tag{3}$$

where Z – vertical, N – north and E – east sensors of the seismic station. Deconvolving the horizontal component with the vertical one we can receive a trace called receiver function, from which the source and instrument characteristics are removed. Additonally, if we consider only the first 100 s of seismogram, the information associated with the propagation of seismic waves in the deep Earth's interior will be removed, too. Finally, the receiver function contains only the information about the seismic structure just beneath the seismic station. The great advantage of the receiver function is the fact that the information about the structure can be obtained based on the single station's recordings only using natural sources of seismic waves, i.e. the earthquakes. So, it is a method relatively cheap and easy compared to seismic reflection or refraction methods. The problem is only to record a sufficient number of seismograms of teleseismic earthquakes to obtain a good directional coverage of seismic rays.

The lithosphere can be defined in different ways, depending on which its properties are investigating. In brief, a rigid layer with increasing velocities of seismic waves with depth – the lithosphere is underlain by a well conductive ductile layer with reduced velocities of seismic waves – the asthenosphere. Seismically thinnest lithosphere, with thickness of 50–100 km, is observed in the "young" and "hot" areas, while in the "old" and "cold" areas it is hardly detected by seismic methods and probably it reaches a depth of 200 km or more. Also the nature of the transition between the lithosphere and the asthenosphere (LAB – litosphere–astenosphere boundary) are discussed. Recent estimates suggest that the LAB is a first order discontinuity (e.g., Eaton et al., 2009). According to the other opinion it is rather a broad transition zone (e.g., Meissner, 1986). The depth of lithospheric roots has important tectonic implications, e.g. a thick cratonic lithosphere increases the thermal insulation of the underlying mantle, which may result in a higher temperature of the mantle and may affect the process of convection (Lenardic et al., 2005; Cooper et al., 2006).

The dynamics of the Earth's mantle is not only effected by the thickness and the depth of LAB, but also by the thickness and the depth of mantle transition zone (MTZ). Investigations of the structure of seismic discontinuities of the MTZ can give the information about temperature changes at the depths of 400–700 km. An existence of transition zone is commonly assigned with phase changes of mantle's minerals (mostly olivine). The fluc-

tuations in depth and thickness of the MTZ are related to the temperature of MTZ (e.g., Bina and Helffrich, 1994). Higher temperatures of the MTZ moves the "410 km" seismic discontinuity (top of the MTZ) down and the "660 km" (bottom of the MTZ) upwards, resulting in thinning of the MTZ. On the contrary, cooling of the MTZ moves the "410 km" up and the "660 km" down, resulting in widening of the MTZ.

Results. Seismic methods using the receiver function, thanks to its extent and relatively good resolution, can effectively explore the structure of the lithosphere and mantle transition zone of Earth. Expanding the basic knowledge about the structure of the interior of Earth and its physical properties is very important from the point of view of the dynamics of the Earth's mantle, and thus the tectonic evolution and processes taking place today on our planet.

Rotation of the receiver function. The correct interpretation and modeling of the receiver function requires a careful choice of coordinate system, in which the recorded seismograms will be presented before the deconvolution operation.

Seismograms are recorded by the seismic station in the ZNE coordinate system, i.e. a direction designated by the local gravity vector (Z – points outside the surface of the Earth), a geographic north-south direction (N – points north) and a east–west direction (E – points east). The ZNE coordinate system is left-handed.

Another commonly used coordinate system is the ZRT coordinate system associated with location of the seismic station and recorded earthquake. The ZRT coordinate system is defined by a vertical direction (the same as for the ZNE), a radial direction designated by the great circle passing through the location of the receiver and the source of earthquake (R – points from the station to the source) and a transversal direction (T) to get right-handed system.

The seismograms can also be presented in the LQT coordinate system, which is associated with the location of station and a plane of polarization of the first (direct) wave recorded by the receiver. The seismic sensor records the sum of three waves: a wave incident on the Earth's surface and longitudinal (P) and shear (S) waves reflected from the Earth's surface. The shear wave generated by the reflection of the longitudinal wave at the seismic discontinuity has the same plane of polarization as the incident wave, so the plane of polarization of recorded signal is the same as the incident wave. A direction of L is determined by the direction of polarization of the recorded first signal i.e. the longitudal wave (P) incident on the Earth's surface (points from the center of the Earth), a Q direction is perpendicular to the L direction in the plane of polarization, a T direction is defined like as in the ZRT coordinate system. The LQT system is right-handed.

A teleseismic P wave has a constant phase velocity and thus can be described as a plane wave. At the seismic discontinuities separating the mediums of different impedances, P wave is reflected and refracted, also as S wave (Fig. 1a). The receiver function is the result of the deconvolution (inverse operation of the convolution) the R component with Z component (RFR) and the T component with Z component (RFT) or/and the Q component with the L component (RFQ) and T component with L component (RFT). The operation of deconvolution can be performed in the frequency domain (e.g., **H1–H3**, Ammon et al., 1990) or in the time domain (e.g., **H4–H5**, Kind et al., 1995). Both methods have their supporters and opponents. For good quality seismograms, both methods give comparable results. In the case of noisy recordings, I have found that the time-domain deconvolution using a Wiener filter (Berkhout, 1977) is more stable than the frequency deconvolution using the water–level method (Clayton & Wiggins, 1976).

When the seismic structure beneath the seismic station consists of a stack of homogeneous layers with horizontal boundaries, in the ZRT and LQT coordinate systems a seismic energy is observed only at the Z and R or L and Q components. Moreover, the RFR contains only the direct P wave and phases associated with the conversion of waves at the seismic discontinuities (PpPms, PpSms, PsPms, etc.), which arrived at the receiver as S waves (Fig. 1b). The RFQ differs from the RFR only by the absence of direct P wave. The delay time of observed phase depends on the depth of seismic discontinuity, where the wave has been converted and the velocity of S wave on the way between the discontinuity and the surface. The amplitude of phase depends on the contrast of impedances at the conversion discontinuity.

In the case of large heterogeneity of the structure beneath the seismic station (e.g. inclined seismic discontinuities and/or significant anisotropy of the medium) a direction of wave's arrival and its slowness may vary for the individual layers. Then, on the RFR all type of waves, e.g. Pp, PpPmp are observed, what makes an interpretation much difficult. Moreover, in that case the amplitudes of RFT are usually comparable with the amplitudes of RFQ and characteristic changes of amplitude's values are observed depending on the direction of wave's arrival.

Usually, an angle necessary for rotation from the ZNE to ZRT coordiante system is calculated based on the known location of seismic stations and the source of earthquake published at seismic bulletins (e.g., **H1–H3**; Ammon et al., 1990; Kind et al., 1995). This angle is determined in relation to the seismic station and is often called a theoretical backazimuth. The real backazimuth of the ray may vary significantly from the theoretical one because of the presence of heterogeneity of the structure beneath the seismic station, i.e. the existence of dipping seismic discontiniuties and/or the seismic anisotropy. In such case the analysis of polarization of the direct P wave at the horizontal components is

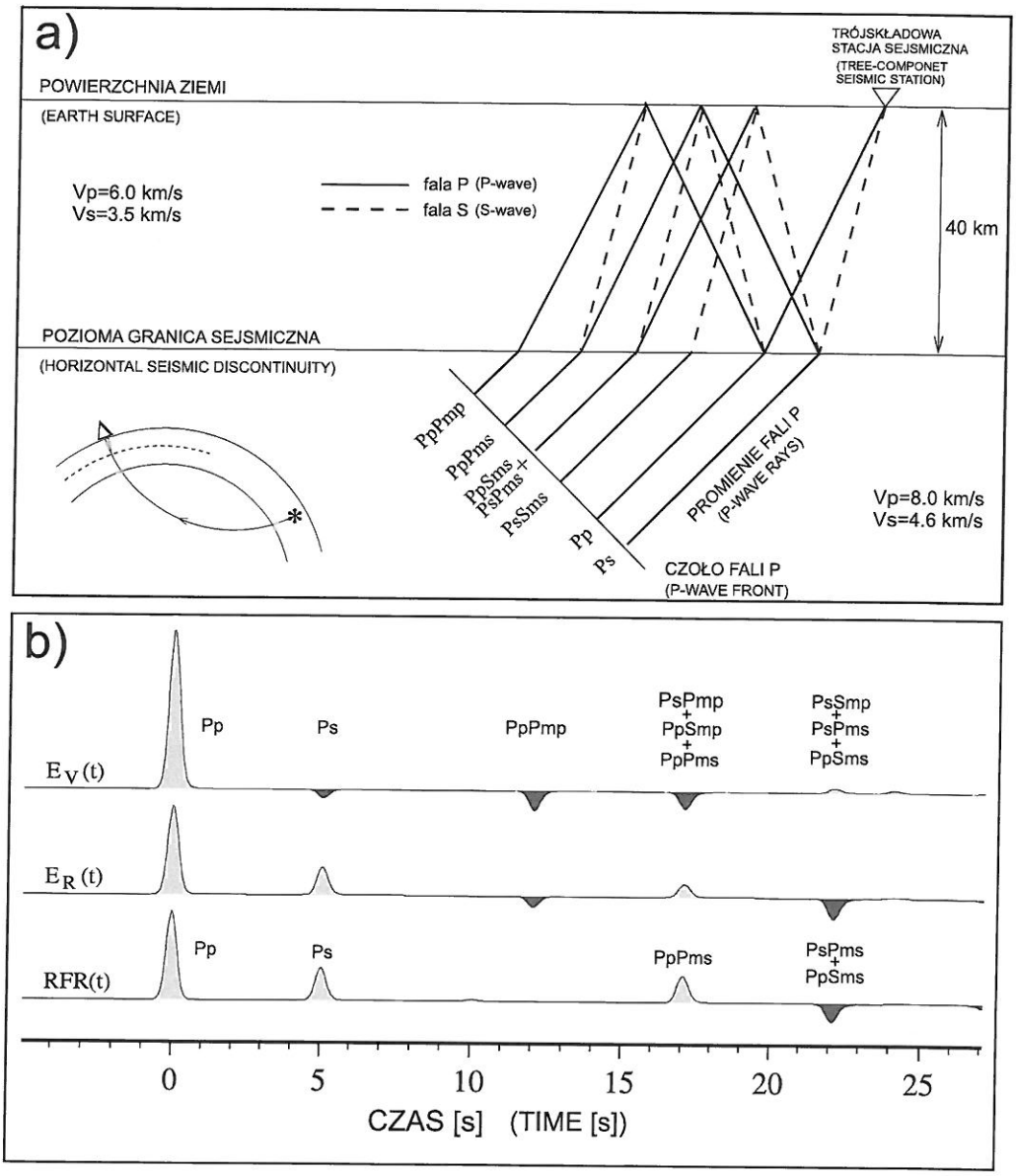

Figure 1: **a)** Refractions and reflections of seismic waves at the seismic discontinuities separating the mediums with different impedances. The solid lines – rays of longitudinal waves (P); the dotted lines – rays of shear waves (S); uppercase letter – waves which are going up; lowercase letter – waves which are going down; "m" – a reflection from the discontinuity; Vp – P-wave velocity, Vs – S-wave velocity. **b)** The vertical (E_V) and radial (E_R) impulse response of the structure for a incoming teleseismic plane P wave and the receiver function (RFR) calculated for the structure shown at a).

necessary (e.g., Jurkevics, 1988; Geissler et al., 2008). Also, the polarization angle necessary for rotation of the seismograms from the ZRT to LQT coordinate system can be determined by applying the above analysis. Another method of determination of the polarization angle is a reduction of the energy of direct P wave at the T component or a determination of eigenvalues of the covariance matrix of the seismogram of direct P wave (e.g., Kind et al., 1995). The polarization angle can be also calculated from the amplitude of RFR at the delay time $t = 0\,\mathrm{s}$ (**H1**; Saul et al., 2000). Above methods (except the last one) define angles of rotation based on the analysis of seismograms. It must be remembered that for individual earthquakes energy distribution recorded by the seismic station can significantly differ from one to another because of the differences of their source function. The receiver function contains only the impulse response of the structure beneath the seismic station, so it is free from that disadvantege. That is the reason why I have proposed the new method of the rotation of seismograms based on the properties of receiver function (**H4**, **H5**).

Due to the definition, the radial receiver function (RFR) contains only the direct P wave (at the delay time $t = 0\,\mathrm{s}$) and waves that have been converted at the seismic discontiniuities. Therefore, the backazimuth can be defined as the direction for which the amplitude of RFR at the delay time $t = 0\,\mathrm{s}$ is highest (maximum). In the case of the structure consisting the stack of horizontal homogeneous layers, that will be correspond to the radial direction (R). Since the seismogram includes the seismic noise, it is better to seek a maximum of energy in a wider time range, not exactly at the time of wave's arrival. In my papers I have proposed two criteria: (1) using a very narrow time interval $t = (-0.05\,\mathrm{s};\ 0.05\,\mathrm{s})$ (**H4**), which is suitable for permanent stations located outside the areas of deep sedimentary basins (lower noise level due to better recording conditions) and (2) using a wide time interval $t = (0\,\mathrm{s};\ 1\,\mathrm{s})$ (**H5**) which is appropriate for temporary stations also located in the areas of deep sedimentary basins (usually for such stations recording conditions are worse than for permanent stations). The sedimentary layers, e.g. on the Polish territory in the Trans-European Suture Zone (TESZ), significantly reduce the amplitudes of direct P wave and increase the amplitudes of waves converted at the shallow discontinuities. Assuming that the uppermost layers have a consistent slope and dip with the Earth's surface, we can determine from them the backazimuth of direct wave P. A procedure of determination of the backazimuth of direct P wave is as follows: we calculate the RFRs from the teleseismic seismogram rotated from the ZNE to ZRT coordinate system with angles from 0° to 360° e.g. every 3°, and then add up amplitudes in the assumed time interval for each RFR. The rotation angle for which the resulting value is the largest (positive) is the searched backazimuth. The seismograms before calculation of the receiver function are filtered with bandpass Butterworth filter with corner preriods of 2 and 10 s to determine the backazimuth of teleseismic waves only. The above method is illustrated

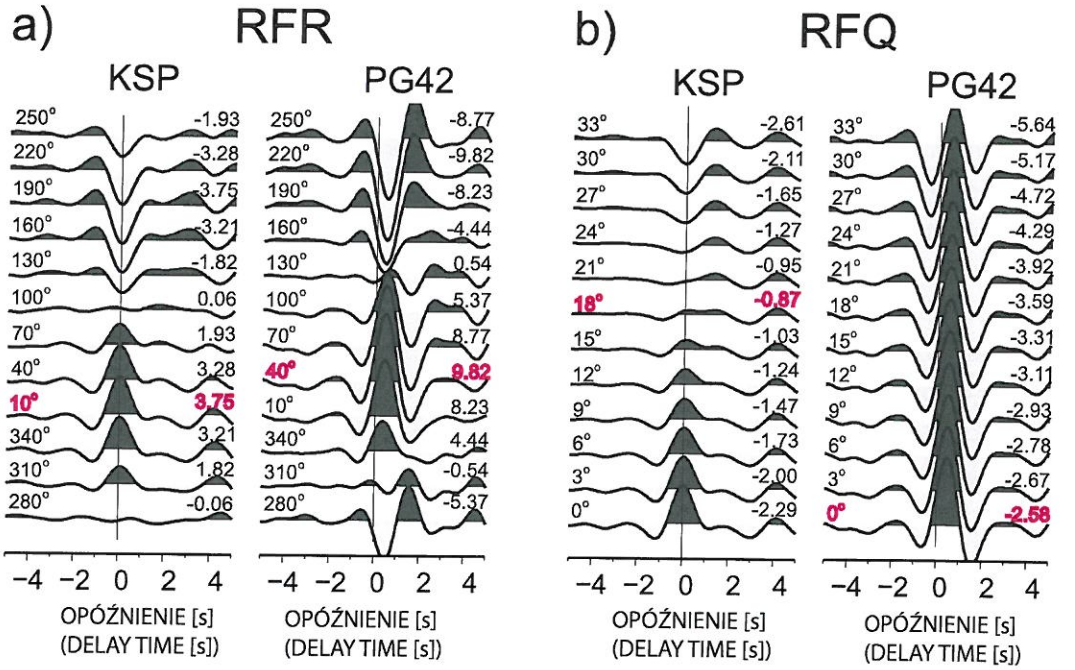

Figure 2: A procedure of rotation of the receiver functon for an earthquake from Aleutian Islands recorded by the permanent seismic station Książ (KSP) and the temporary seismic station Sajdak (PG42). **a)** the RFRs calculated from the seismograms rotated from the ZNE to ZRT coordinate system every 30^o (numbers to the left) and sums of amplitude in a time interval $t = (0\,\mathrm{s};\ 1\,\mathrm{s})$ (numbers to the right); **b)** the RFQs calculated from the seismograms rotated from the ZRT to LQT system every 3^o (numbers to the left) and sums of negative amplitude in a time interval $t = (-2\,\mathrm{s}, 0\,\mathrm{s})$ (numbers to the right). The search backazimuth and polarization angles of direct P wave and value of parameters used to their estimation are marked in red (**H5**).

in Fig. 2a.

We can similarly proceed with a determination of the polarization angle of direct P wave. We rotate the seismogram from the ZNE to ZRT coordinate system using earlier determined backazimuth angle, and then calculate the RFQs from seismograms rotated from the ZRT to LQT coordiantes system with the polarization angles from 0° to 45° every e.g. 1°. In the absence of seismic noise, in the LQT coordinate system the seismic energy on the Q component for the direct P wave should be zero. Unfortunately, if there are strong contrasts of impedance at shallow depth just beneath the seismic station, part of the energy of the waves converted at the near-surface discontinuities is observed on the RFQ at the time $t = 0\,\mathrm{s}$. Therefore, in the time range $t = (-2\,\mathrm{s}, 0\,\mathrm{s})$ we minimize the seismic energy at the RFQ by calculation a sum of negative amplitudes. Then we look for the polarization angle for which the difference of successive sums becomes negative. In

addition, to take into account the existence of seismic noise, we calculate for each RFQ a sum of power of amplitudes within a given range. If this value reaches its minimum and the difference of the sum of negative amplitudes will not be negative at this time, the calculations are interrupted and the polarization angle is assumed to be that from previous step. The above procedure is illustrated in Fig. 2b.

The presented procedures are not numerically time-consuming and are automatic, what is their huge advantage over previously used methods of the determination of the rotation angles. Additionally, I have successfully tested them with synthetic RFs calculated for theoretical models, in which the medium consists of a homogeneous layer with dipping bottom, a homogeneous layer with dipping top (the Earth's surface) and with a thin homogeneous layer with low seismic velocities overlying it (**H5**). For above calculation I have written a code that modified the ray-tracing method presented by Langston (1977b) to take into account the inclination of the Earth's surface. The program was an extension of the code, I have used in the PhD dissertation.

I have applied the presented procedures of the rotation of teleseismic seismograms to the recordings of permanent stations located on the Svalbard Archipelago on the metamorphic basement of the Caledonian orogeny covered by Paleozoic and youger sediments (**H4**) and to the recordings of permanent and temporary stations on the Polish territory, situated on the Precambrian Platform, in the TESZ and on the Paleozoic Platform (**H5**). Rotations angles calculated by my method did not differ significantly from the theoretical ones (**H5**), because at the above areas no signifiant heterogeneity of near-surafce layers are observed. The additional advantage of the described method is that possible incorrect orientation of seismic sensors to the north, is automatically corrected, it could be unknown and had not to taking into account during the rotation as it is necessary in the case of using theoretical backazimuth.

Selection of receiver function. In order to improve the signal-to-noise ratio, receiver functions for each station are stacked in distance and/or backazimuth bins. The size of bins are determined individually for each station and they are related to the variability of receiving function, as well as the amount of used data. Usually, the mean (stacked) receiver function is used and it is calculated from all teleseismic seismograms recorded by seismic station. However, before stacking the receiver functions, it is necessary to assess their quality. Not for everyone seismogram, calculated receiver function contains only the impulse response of the structure beneath the seismic station. It depends on e.g. the complexity of the source function, especially when the source emits waves for a time longer than used in calculations. Ammon (1991) in his theoretical considerations about the receiver function, has assumed that the source function of earthquake is a Dirac delta function. Also waves

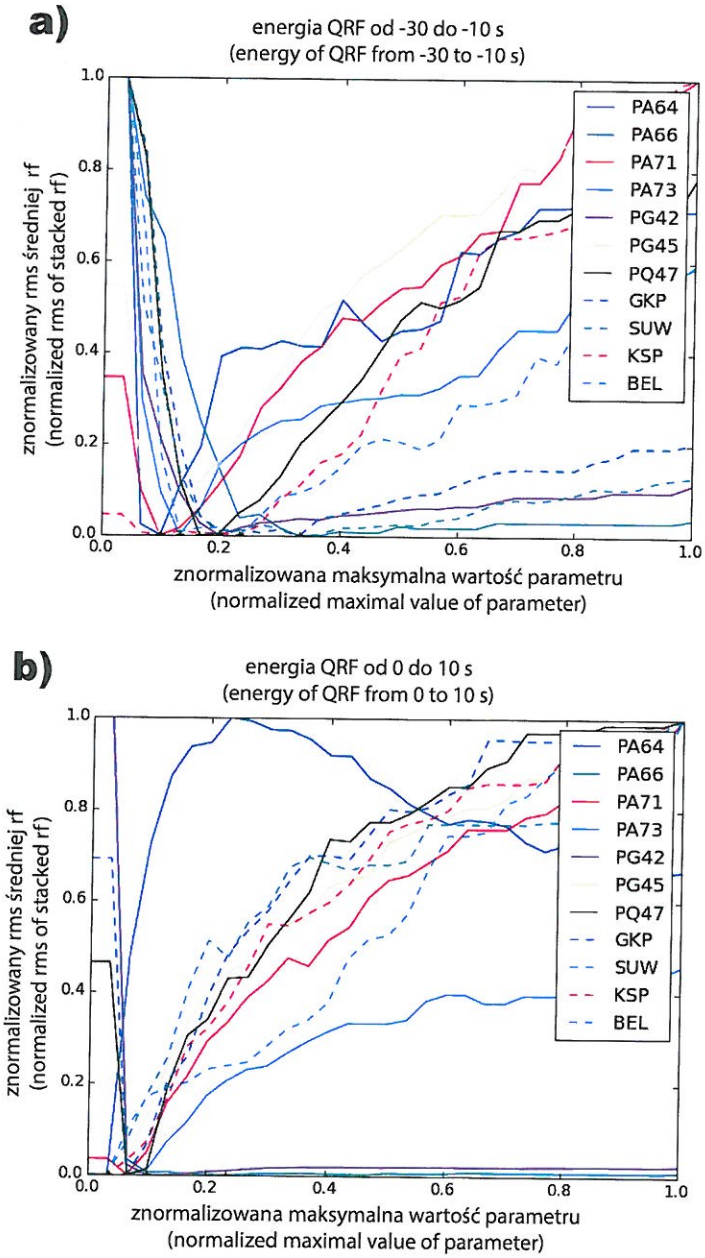

Figure 3: The normalized distribution of rms of stacked receiver function selected based on parameters: **a)** the total energy of RFQ in the time range t=(-30 s; -10 s) and **b)** the total energy of RFQ in the time range t=(0 s; 10 s).

incoming to the station from the source within the first 100 s, which are not the result of conversion of the direct P wave at seismic discontinuities beneath the station, can disturb

the receiver function. Routinely, the quality assessment of seismograms for the receiver function calculation is done by visual verification, also the evaluation of calculated receiver function is subjective and depends on the experience of researcher. To find an objective criteria of the receiver function selection, I have tested various parameters characterizing the receiver functions e.g.: energy of the RFQ, RFR and RFT recorded in the different time interval; the maximum amplitude of the RFL (deconvolution of the L component with itself in the case of a well defined Wiener filter should be a Dirac delta function), RFQ, RFR and RFT; the maximum absolute value of Fourier transform of the RFQ, RFR and RFT in the different period interval. The distribution of root mean square (*rms*) of the stacked receiver functions selected based on 10 parameters have minima or maxima that allow for the determination of their optimal values. The examples of the distribution of rms for the permanent and temporary seismic stations from the Polish territory for two parameters are shown in Fig. 3.

I have applied above method of receiver function selection to the receiver functions of permanent seismic stations of the Svalbard Archipelago (**H4**). Used parameters and their ranges are shown in Table 1. The presented method allows for the fast and objective selection of the best receiver functionis, e.g. in the case of the Ny-Alesund seismic station (KBS) 823 receiver functions among 2258 meet the required quality criteria.

Table 1: The list of the parameters and their values used for the RFQ and RFT selection

Parameter's Name	Parameter' Type	Min. Value	Max. Value	Range Value	Component used in calculations
ex0a	maximal amplitude	0,0	0,3	(-80 s; -1 s)	absolute value of LRF
ex0b	maximal amplitude	0,0	0,3	(1 s; 80 s)	absolute value of LRF
ex1	rms	0,0	0,04	(-70 s; -30 s)	QRF, TRF
ex2	rms	0,0	0,04	(-30 s; -10 s)	QRF, TRF
ex3	rms	0,0	0,04	(-10 s; 0 s)	QRF, TRF
ex4	rms	0,04	0,1	(0 s; 10 s)	QRF, TRF
ex5	rms	0,02	0,08	(10 s; 30 s)	QRF, TRF
ex6	rms	0,01	0,05	(30 s; 70 s)	QRF, TRF
ex8	rms	0,02	0,07	(-70 s; 70 s)	QRF, TRF
ex9	maximal amplitude	0,0	5,0	(0,01 Hz; 0,03 Hz)	absolute value of QRF and TRF

Modelling of the lithospheric structure by the trial-and-error method. Modelling of the lithospheric structure by a trial-and-error method based on the receiver function is not often used technique due to its time-consuming and the difficulties arising from the proper

assessment of individual phases present in the observed receiver function. This method, however, allows to obtain additional valuable informations about the distribution of shear waves with depth beneath the seismic station or to verify the results of inversion methods. In order to objectify the modelling procedure by using reliable starting model, at the paper **H4** I have proposed to determine the near-surface S-wave velocity based on the amplitude of the RRF (Saul et al., 2000) and thickness and average Poisson's ratio of the crust (Zhu and Kanamori, 2000).

Estimation of near-surface S-wave velocity. The main problem in the receiver function modelling is the nonuniqueness of informations contained therein. A delay time of recorded waves converted at the seismic discontinuities beneath the station with respect to the direct P wave depends on the depth of the discontinuity and the average seismic velocity on the way between the discontinuity and the station. For the first time this problem has been reported by Ammon et al. (1990). Saul et al. (2000) have proposed to determine the value of the near-surface S-wave velocity beneath the seismic stations based on the measurement of amplitudes of RFR at the time $t = 0\,\mathrm{s}$ and to use it in the modelling procedure. Assuming that the medium consists of flat homogeneous layers, the amplitude of RFR at the time $t = 0\,\mathrm{s}$ depends only on the slowness and the near-surface S-wave velocity (Kennett, 1983):

$$RFR(0) = \frac{2p\sqrt{\frac{1}{V_s^2} - p^2}}{\frac{1}{V_s^2} - 2p^2}, \tag{4}$$

where $RFR(0)$ – the amplitude of RFR at $t = 0\,\mathrm{s}$, p - the slowness parameter, V_s – the near-surface S-wave velocity. So, the near-surface S-wave velocity is given by formula (Wachnicka, 2005):

$$V_s = \frac{1}{p}\sqrt{\frac{1}{2} - \frac{1}{2\sqrt{RFR(0)+1}}}. \tag{5}$$

By measuring the $RFR(0)$ for each earthquake we can determine the distribution of near-surface S-wave velocity, as well as an average value for the station. I have esimateted the mean value of near-surface S-wave velocity for the seismic stations from the Bohemian Massif and it was 3.19–3.87 km/s (**H1**), and for the seismic stations located on the Svalbard Archipelago — 1.7 ± 0.8; 1.7 ± 0.6 and 1.0 ± 0.5 km/s with uniform backazimuth distribution (**H4**).

The determination of the depth of Moho discontinuity and the average Poisson's ratio of crust. The receiver function analysis can also be used to determine the thickness and average Poisson's ratio of crust if the converted and multiple reflected waves from the Moho

discontinuity and the Earth's surface are observed. Zhu and Kanamori (2000) have proposed a method in which the amplitude of converted wave at the Moho discontinuity and its multiple reflections are stacked due to the delay times estimated for different values of thickness (H) and Poisson's ratio (σ) of the crust. The pair of parameters (H, σ), which shows the greatest coincidence for all events recorded by the seismic station is sought/optimal set. Using this method to the recordings of seismic stations from the Svalbard Archipelago I have received the following values of thickness and average Poisson's ratio of the crust: $(25 \pm 3$ km$, 0.28 \pm 0.07)$ for the KBS station (northern Spitsbergen); $(32 \pm 3$ km$, 0.21 \pm 0.08)$ for the HSPB station (southern Spitsbergen) and $(33 \pm 3$ km$, 0.24 \pm 0.08)$ for the SPITS seismic array (central Spitsbergen).

I have used the above informations to model the seismic struture by trial-and-error method – the S-wave velocity distribution down to the depth of 150 km in the area of Svalbard Archipelago (**H4**). The receiver functions of seismic stations in southern and central Spitsbergen show that the lower lithosphere at the depth of 50–100 km has the structure consists of stack of layers with normal and reduced S-wave velocity with respect to the one-dimensional global model IASP91 (Kennett and Engdahl, 1991), while the lower lithosphere of northern Spitsbergen shows no such variation (**H4**). Czuba (2013) has observed on the refraction profiles (P waves) the existence of reflecting discontinuties in the lower lithosphere at the depths of 40–50 km in the central and southern parts of Spitsbergen. Also, the analysis of surface waves made by Levshin et al. (2007) shows a large horizontal and vertical diversity of S-wave velocity at the depth of 40–15 km in the central and the southern parts of the Svalbard Archipelago.

Linearized inverse modelling of the structure of lithosphere. In the linearized inverse method we are linearizing the relationship between the model (distribution of S-wave velocity with depth) and the corresponding receiver function (e.g., Ammon et al., 1990). Starting from a initial model we are iteratively improving it by minimizing an objective function, which is a function of difference between the receiver function calculated from the model and observed one. An important numerical process in inverse modeling is to minimize the objective function, which is a function defined in terms of the difference between the collected field seismic data and the numerically computed seismic data.

The starting model should be closed to the real structure to meet the assumption of linearity. The medium is modelled by the stack of flat homogeneous layers with constant thickness. Unfortunately, the result of linearized inversion depends strongly on the choice of initial model. Ammon et al. (1990) have taken as the initial models modified refraction models (P-wave velocity) and have inverted the radial receiver function (RFR). In order to

reduce the nonuniqueness of receiver function inversion, they have proposed the using of *a priori* informations to reject the models with the significant deviation of S-wave velocity from the expected ones. Unfortunately, not always *a priori* informations are available, Besides, the S-wave velocity distribution not necessarily must be complimentary to the P-wave velocity distribution. In order to obtain the reliable S-wave velocity distributions based on the linearized inversion of receiver function, I have proposed to run inversion with many simple starting models with the wide range of the S wave velocities, the thickness of the sediments and cristalline crust, and finally to average the resulted models. In the paper **H1** I have calculated and analyzed the RFR and RFQ of permanent seismic stations from the area of the Bohemian Massif. I have considered three classes of starting models to test the sensitivity of linearized receiver function inversion on different elements of the structure: the contrast of seismic velocity at the Moho discontinuity, the velocity gradient in the crust and sediment layer with low seismic velocities. I have run the inversion of RFR and RFQ, respectively. Results of modelling show that all three classes of starting models converged to the nearing S-wave velocity distribution. However, the inversion of RFQ gives much more stable results in the lower lithosphere than the RFR, which gives for all stations very low S wave velocities (< 4.0 km/s). Fig. 4 shows one-dimensional S-wave velocity distributions, which I have received by the linearized inversion of the RFQ of seismic stations from the area of Bohemian Massif.

Inverse modelling of the lithospheric structure by the Monte Carlo method. Monte Carlo methods (MCMs) are widely used to solve inverse problems, not only in seismology, but wherever the relationship between the recorded data and the searched model is non-linear. That is the case of receiver function. The main problem of all MCMs is their time-consuming. But nowadays, even personal computers are powerful enough to cope with calculations needed in the MCM within an acceptable time. Therefore since the late 90's number of researchers using MCMs has increased exponentially.

In the paper **H3**, the MCM are used together with the neighborhood algorithm (Sambridge, 1999a,b). This algorithm can be easily adapted to geophysical problems and can be combined with other algorithms. What more, it speeds up calculations and selection of its parameters is not difficult. The inverse modelling of the lithospheric structure by the MCM has been applied to the radial receiver function (RFR) — the same which were inverted by the linearized method for permanent seismic stations located in the area of the Bohemian Massif in the paper **H1**. The models obtained by the MCM inversion provide stable results down to the depth of 70 km, though the RFR was inverted. Layers with the low S wave velocities in the middle crust visible in the models obtained by the linearized inversion, are not so pronounced in the MCM models. It appears also that they are not

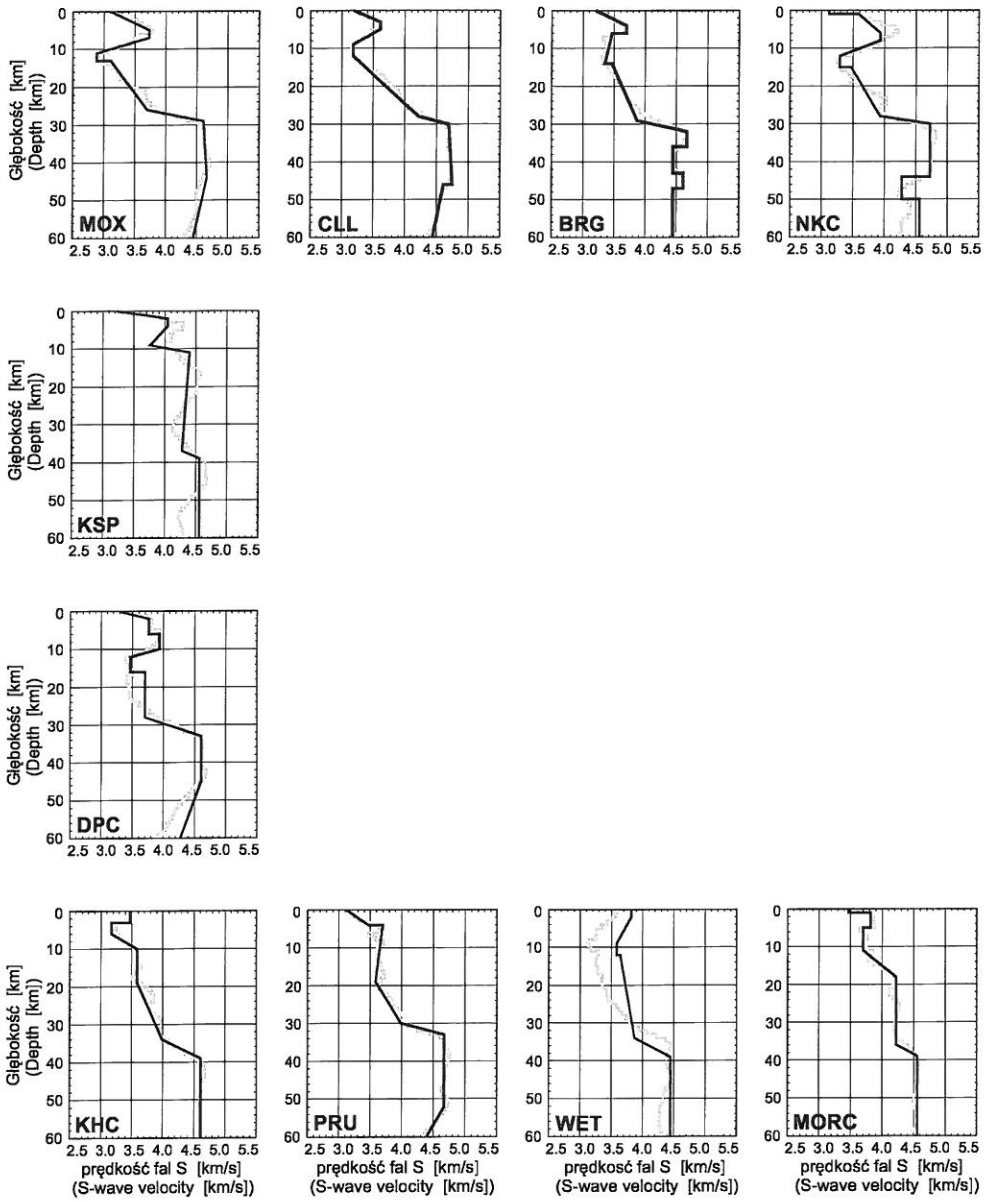

Figure 4: The S-wave velocity distributions obtained by the trial-and-error modelling (black lines) and the linearized inversion (gray lines) of the area of Bohemian Massif. The observed receiver functions are marked by dashed lines and theoretical ones caluculated for final models are marked by solid lines (**H1**).

the result of modelled high-velocity layers above them. This is a typical problem in the linearized inversion — large contrasts of seismic velocities in the linearized inversion must

be modelled by velocity gradient and broad zone. An additional advantage of the MCMs is the information about the ratio of P and S velocities (Vp/Vs), which is also inverted. In the linearized method, the Vp/Vs ratio must be assumed and are not changed during the inversion. The inversion modelling by MCMs has significantly improved the estimation of the distribution of S-wave velocity at the lower lithosphere in the area of the Bohemian Massif. The MCM inversion was made by Jacek Trojanowski in his Master thesis which I was a supervisor (Trojanowski, 2007).

Determination of the depth of seismic discontinuities in the transition zone of Earth's mantle. Based on the receiver function we can also receive an information about the deeper layers of Earth's mantle. Thanks to migration methods and advanced methods of seismic data visualization, the mapping of discontinuities associated with the mantle transition zone (MTZ), i.e. the "410 km" and "660 km" is possible (e., Kosarev et al., 1999; Poppeliers and Pavlis, 2003). The sections (profiles) of receiver function can be presented in the time or depth domain by using a reference velocity model. The amplitudes of converted waves at the discontinuities of MTZ are very week, an order of magnitude smaller than those from the Moho discontinuity. To observe such a weak signal, the receiver functions must be add up in special way. For this, each receiver function is shifted in time based on the reference model, e.g. IASP91 (Kennett and Engdahl, 1991), as each point was the converted wave with the slowness of $6.4s/^o$. Next, the same reference model is used to calculate the path of seismic rays. In this way we can estimate the coordinate (latitude and longitude) of conversion point (piercing point) at the tested discontinuity in reference to the seismic station. That allows us to group/sum receiver functions due to the piercing points. In the paper **H4** I have used this method to determine the depth of the "410 km" and "660 km" discontinuities in the area of Svalbard Archipelago. The receiver functions were summed up in the bins of size of 9° (longitude) and 2° (latitude). The delay times of wave converted at the "410 km" discontinuity comparing to the IASP91 global model show no deviations for the northern and central part of Svalbard Archipelago, while for the southern parts they are significantly shorter. The delay times of waves converted at the "660 km" discontinuity are the same as in the IASP91 global model for the northern part of Svalbard Archipelago, but for the central and southern parts the differentiation is evident between the western (times longer) and the eastern part of archipelago (shorter times). The latest regional model of shear wave velocity of European plate determined based on the surface wave analysis done by Legendre et al. (2012) very well explains the observed delay times of converted waves at the "410 km" discontinuity. But, it does not explain the delay time of converted waves at the "660 km", which allowed me to hypothesize that the MTZ of the western part of Svalbard Archipelago is thicker and the eastern part is thinner

comparing to the results of surface wave tomography.

We can also plot the amplitudes of receiver function along the path of seismic rays (seismic migration) in the depth domain. The two-dimensional projection along the vertical profile allows to map the shape of discontinuities at which the seismic waves are converted. I have made such cross-section based on the recordings of seismic stations operating during the POLONAISE'97 (Guterch et al., 1999) and SUDETES 2003 experiments (Grad et al., 2003b) along the P4 profile (Grad et al., 2003a) running from the south-west to north-east Poland (**H3**). It shows that the thickness and the depth of MTZ in the area of north-east Poland do not differ significantly from the IASP91 global model. Contrary, in the area of south-west Poland, the MTZ is much thinner and located deeper than in the IASP91 global model. These results are consistent with the tectonic scheme and the heat flow measurements of Polish territory. In warmer area (young) the MTZ is thinner and more deeply situated than in the colder (old) areas (Bina and Helffrich, 1994).

Summary. The receiver function analysis is a very useful tool in the study of seismic structure of the crust and mantle. It requires only the recordings of teleseismic earthquakes (seismograms) recorded by the single three-component seismic station, premanent one (seismological observatory) as well as temporary one (passive seismic experiments). The use of different techniques of receiver function enables to investigate the seismic structure beneath the seismic station, to identify the seismic discontinuities and to estimate their depths and the distributions of S-wave velocity. The refraction methods give a very good estimation of P-wave velocity distributions, however S waves usually are not well recorded, so it is difficult to obtain from them the S-wave velocity distribution. The models received based on the surface wave analysis have much worse resolution than those obtained from the receiver function.

5. Discussion of other scientific achievements

5.1. Achievements obtained before the PhD degree

Master thesis. A Master's thesis in the physics of lithosphere I have written under the supervision of prof. Marek Grad at the Institute of Geophysics, Faculty of Physics, University of Warsaw (Wilde-Piórko, 1997). The subject of my thesis was modelling of the seismic structure based on the receiver function analysis of the first Polish broadband seismic station Suwałki (SUW) which began operation at the end of 1995. I cataloged seismograms of teleseismic earthquakes recorded by the Suwałki station. Then I have calculated the radial and transversal receiver functions using simultaneous deconvolution in the frequency domain. I have used a program written by myself to determine the one-dimensional distri-

bution of S-wave velocity beneath the seismic station by the linearized inversion method. The inversion has been run for three simple starting models. In result I have estimated the first distribution of S-wave velocity beneath the SUW station.

Interpretation of the regional and teleseismic earthquakes recorded during the passive part of POLONAISE'97 experiment. During POLONAISE'97 – the active seismic experiment (Guterch et al., 1999) twenty Polish short-period seismic stations were continuously recording the ground motion for three months along the P4 profile (Grad et al., 2003a) in the area of central Poland. I have chosen for further analysis seismograms of three regional events located at the vicinity of Lubin and estimated for them traveltimes of P (longitudal) and S (shear) waves with respect to the IASP91 global reference model (Kennett and Engdahl, 1991). I have carried out the same analysis for ten seismograms of teleseismic earthquakes with good recorded signal-to-noise ratio. Additionally, I have calculated from the teleseismic seismograms radial and transversal receiver functions of each station. The time residues of seismic waves, as well as the receiver functions plotted along the seismic profile clearly show the large diversity of the Earth's crust on the Polish territory — especially it is well visible the deep sedimentary basin in central Poland (Wilde-Piórko et al., 1999).

PhD thesis. My PhD thesis has refered to the modelling of the structure of crust and uppermost mantle in the area of south Sweden, Denmark and north Germany, as well as north–east Poland and south Germany based on the receiver function analysis (Wilde-Piórko, 2002a; Wilde-Piórko et al., 2002b). My investigations have enclosed the analysis of seismograms of teleseismic earthquakes recorded by the twenty eight temporary broadband stations of passive seismic experiment TOR (Gregersen et al., 1999). For each seismic station (one year of continuous recording) I have calculated the stacked (mean) radial receiver function using the deconvolution in the frequency domain and then inverted them by the linearized algorithm for one class of starting models (constant S-wave velocity in the crust and uppermost mantle). The results I have interpolated along the vertical profile to plot the two-dimensional distribution of S-wave velocity down to the depth of 60 km. I have also estimated the two-dimentional distribution of ratio of P- and S-wave velocity (Vp/Vs) using the P-wave velocity destribution along the analyzed profile (Arlitt et al., 1999). Additionaly, due to the long period of recordings of the permanent Suwałki station (SUW) and the Mox (MOX) stations I have calculated the backazimuthal distributions (sections) of receiver function (RFR and RFT). This way I could carry out the 2.5-D modelling of the structure beneath the seismic stations. I have calculated using a program written by myself the synthetic receiver functions for medium consisted with a stack of homogeneous

layers with any boundary's strike and dip and the assumption that the Earth's surface is flat. By the trial-and-error method, comparing the synthetic backazimuth sections of receiver function with observed ones, I have found that there is a layer of reduced S-wave velocity in the middle crust of south Germany, which strike coincides with the direction of stress field in this area. For north-east Poland, the dominant feature of crust is a thin layer of sediments with very low S-wave velocity, directly overlying the crystalline crust. So, the receiver functions are dominated by waves which are repeatedly reflected from the sediement-crystalline crust discontinuity and the Earth's surface.

5.2. Achievements obtained after the PhD degree

Modelling of the structure of crust of the polar regions. In the framework of international cooperation with the Alfred Wegener Institute (AWI) in Bremerhaven I have analyzed seismograms of teleseismic earthquakes recorded by the short-period seismic stations located in Eastern Antarctica. Based on the receiver function analysis the distributions of S-wave velocity down to the depth of 60 km for the WAZ and OLY stations were estimated by the trial-and-error method. In the case of the OBS station located on a ice floe, only the thickness of the ice was estimated. A layer of water has cut off all waves converted from P to S at the deeper discontinuities — in a liquid medium the S (shear) waves do not propagate. The calculation and modelling of receiver functions was made by Alexandra Wachnicka in her Master thesis which I was a supervisor (Wachnicka, 2005).

During the 4th International Polar Year at the Polish Polar Station in Horsund, the Svalbard Archipelago, the broadband seismic station (HSPB) was installed. As a member of the Polish–Norwegian team I have analyzed the recordings of teleseismic earthquakes of the HSPB seismic station. Though not a very long time of station operation (1.5 years), I have managed to find the dipping seismic discontinuity in the upper crust based on the analysis of the backazimuthal sections of receiver function (RFQ and RFT) — the discontinuity, which was not indentified previously on the refraction profile (Czuba et al., 2008).

Modelling of the potential fields. After my PhD study I was also interested in the analysis of potential fields, the gravity and magnetic fields of the north-east Poland, where the Kętrzyń intrusion is located. The modelling of gravity field based on the 3-D seismic tomographic model (Czuba et al., 2002), as well as testing the relationship between the obtained magnetic model and gravity field have been made. The optimization procedure was applied to the gravity modelling, i.e. the relation function was sought with some phenomenological limits of its value, to get the best fit of the modelled field and the observed one. Finally, no correspondence between the modelled and observed fields was received, what was not the result of incorrect modelling procedure, but most likely it was the result

of inadequate assumption of the morphology of high velocity body in seismic studies. The Kętrzyń intrusion is built with anorthosite surrounded by diorite. The diorite boundary most probably strongly refracted seismic waves, so seismic ways did not penetrate the interior of intrusion (anorthosite). The modelling of magnetic field of the Kętrzyn intrusion was performed with the magnetization parameters of well recognized sister intrusion — Suwałki. As a result, the relatively good fit for the central part of investigation area was received, despite very complex image of magnetic field and very large residual magnetization of intrusion. The modelling of potential fields was made by Magdalena Kłaczkowska in her Master thesis which I was a supervisor (Kłaczkowska, 2006).

Spectral analysis of recordings of teleseismic earthquakes. Recordings of teleseismic earthquakes can also be used to analyze the frequency content of earthquake's source function. In the paper Wilde-Piórko et al. (2011a) and Wilde-Piórko et al. (2011b) I have calculated the spectral seismograms of Sumatra-Andaman earthquake from the recordings of 480 broadband seismic stations located aroung the globe. I have confirmed, among other things, that based on the analysis of spectral seismograms, we can distinguish for the Sumatra–Andaman earthquake a sequence of four separate stages of the rupture of medium along the fault. Each stage had a different maximal frequency of recorded waves and the length of duration. The estimated total time of the whole process was about 540 seconds. The maximal frequencies of recorded waves showed also the azimuthal dependency. The above results are consistent with previously published analysis of the earthquake's source mechanism obtained based on the near-field recordings.

Local seismicity of the area of Poland. Natural seismicity of the area of Poland is very poor. So, to detect it a dense network of seismic stations is necessary. Unfortunately, at that moment in Poland only 8 permanent seismic stations of the Polish Seismological Network are operating. Passive seismic experiments provide opportunities to explore the local seismicity in the area with poor coverage of permanent stations. During 2006–2008 two hundred seismic stations were continuously operating in the territory of south-east Germany, Czech Republic, Poland and Lithuanian in the framework of passive seismic PASSEQ 2006–2008 experiment (Wilde-Piórko et al., 2008). I was a co-organizer and a main coordinator of this experiment, and an executive coordinator in Poland. The recordings of PASSEQ 2006–2008 seismic stations have allowed for a detection and location of four previously unknown seismic events: three in the Baltic Sea, and one in the vicinity of Jarocin. The detection and location of seismic events were made by Marcin Polkowski in his Master thesis which I was a supervisorn (Polkowski, 2012; Polkowski et al., 2016).

Determination of the orientation of seismic stations based on the Rayleigh waves polarization analysis. A three-component seismic sensor should be oriented like as one of its horizontal component should point to the north pole of the Earth. However very often, it is set imprecisely and then the data recorded by the station must be corrected. A true orientation of sensor can be determined based on the analysis of the polarization of Rayleigh waves recorded by the seismic station. Maria Grycuk in her Bachelor thesis (Grycuk, 2015), written under my supervision, has examined seismograms recorded by 26 broadband seismic stations located on the Polish territory, which were operating continuously for two years in the framework of the PASSEQ 2006–2008 experiment (Wilde-Piórko et al., 2008). A program written by Maria Grycuk automatically estimated the angle by which the seismograms should be corrected (rotated).

Joint inversion of the receiver functions and dispersion curves. Last year I have interested in the joint inversion of the receiver function and dispersion curves of surface waves. By enabling the surface waves into the modelling, the results of inversion (distribution of S-wave velocity) are improved. Based on the analysis of the dispersion curves of surface waves the absolute S-wave velocity in the lithosphere and astenosphere can be determined. Unfortunately, the surface waves have much longer periods, so they have much poorer horizontal resolution than the receiver function. The joint inversion of the receiver functions and dispersion curves can eliminate the trade off between layer's thickness and the average seismic velocity. Kajetan Chrapkiewicz in his Master thesis, written under my supervision, now perform the joint linearized inversion of the receiver function and dispersion curves down to the depth of 250 km based on the recordings of broadband seismic stations of the "13 BB Star" exteriment in the area of north-west Poland (Grad et al., 2015; Wilde-Piórko et al., 2016).

6. Reference

Ammon, C.J., Randall, G.E., Zandt, G., 1990. On the Nonuniqueness of Receiver Function Inversions, *J. Geophys. Res.*, **95**, 15303–15318.

Ammon, C.J., 1991. The isolation of receiver effects from teleseismic P waveforms, *Bull. seism. Soc. Am.*, **81**, 2504–2510.

Arlitt, R., Kissling, E., Ansorge, J., TOR Working Group, 1999. Three-dimensional crustal structure beneath the TOR array and effects on teleseismic wavefronts, *Tectonophysics*, **314**, 309–319.

Berkhout, A.J., 19977. Least square inverse filtering and wavelet deconvolution *Geophysics*, **42**, 1369–1383.

Bina, C.R., Helffrich, G., 1994. Phase transition Clapeyron slopes and transition zone seismic discontinuity topography, *J. Geophys. Res.*, **99**, 15853—15860.

Clayton, R.W. & Wiggins, R.A., 1976. Source shape estimation and deconvolution of teleseismic bodywaves, *Geophys. J. R. astr. Soc.*, **47**, 151–177.

Cooper, C.M., Lenardic, A., Moresi, L., 2006. Effects of continental insulation and the partitioning of heat producing elements on the Earth's heat loss, *Geophys. Res. Lett.*, **33**, L13313.

Czuba, W., 2013. Seismic view on the Svalbard passive continental margin, *Acta Geophysica*, **61**, 1088-–1100.

Czuba W., Grad M., Luosto U, Motuza G., Nasedkin V., POLONAISE P5 Working Group, 2002. Upper crustal seismic structure of the Mazury complex nad Mazowsze massif within East European Craton in NE Poland, *Tectonophysics*, **360**, 115–128.

Czuba, W., Grad, M., Guterch, A., Majdański, M., Malinowski, M., Mjelde, R., Moskalik, M., Środa, P., Wilde-Piórko, M., Nishimura, Y. 2008. Seismic crustal structure along the deep transect Horsted'05, Svalbard, *Pol. Pol. Res.*, **29**, 279-–290.

Eaton D.W., Darbyshire F., Evans R.L., Grütter H., Jones A.G., Yuan X., 2009. The elusive lithosphere- asthenosphere boundary (LAB) beneath cratons, *Lithos*, **109**, 1–22.

Geissler, W.H., Kind, R., Yuan, X., 2008. Upper mantle and lithospheric heterogeneities in central and eastern Europe as observed by teleseismic receiver functions, *Geophys. J. Int.*, **174**, 351–376.

Grad, M., Jensen, S., Keller, G.R., Guterch, A., Thybo, H., Janik, T., Tiira, T., Yliniemi, J., Luosto, U., Motuza, G., Nasedkin, V., Czuba, W., Gaczyński, E., Środa, P., Miller, K., Wilde-Piórko, M., Komminaho, K., Jacyna, J., Korabliova, L., 2003a. Crustal structure of the Trans-European Suture Zone region along POLONAISE'97 seismic profile P4, *J. Geophys. Res.*, **108**, 2541-–2565.

Grad, M., Polkowski, M., Wilde-Piórko, M., Suchcicki, J., Arant, T., 2015. Passive seismic experiment "13 BB star" in the margin of the East European craton, northern Poland. *Acta Geophysica*, **63** 2, 352–373.

Grad, M., Špičák, A., Keller, G.R., Guterch, A., Brož, M., Hegedüs, E., Working Group, 2003b. SUDETES 2003 Seismic experiment, *Stud. Geophys. Geod.*, **47**, 681-–689.

Gregersen, S., Pedersen, L.B., Roberts, R.G., Shomali, H., Berthelsen, A., Thybo, H., Mosegaard, K., Pedersen, T., Voss, P., Kind, R., Bock, G., Gossler, J., Wylegalla, K., Rabbel, W., Woelbern, I., Budweg, M., Busche, H., Korn, M., Hock, S., Guterch, A., Grad, M., Wilde-Piórko, M., Zuchniak, M., Plomerova, J., Ansorge, J., Kissling, E., Arlitt, R., Waldhauser, F., Ziegler, P., Achauer, U., Pedersen, H., Cotte, N., Paulssen, H., Engdahl, E.R., 1999. Important Findings Expected From Europe's Largest Seismic Array, *EOS Trans. AGU*, **80**, 1, 6.

Grycuk, M., 2015. Wyznaczanie orientacji stacji sejsmicznych eksperymentu PASSEQ 2006-2008 na podstawie polaryzacji fal Rayleigha, *Bachelor's thesis*, University of Warsaw, Warsaw.

Guterch, A., Grad, M., Thybo, H., Keller, G.R., POLONAISE Working Group, 1999. POLONAISE'97 — international seismic experiment between Precambrian and Variscan Europe in Poland, *Tectonophysics*, **314**, 101–121.

Jurkevics, A., 1988. Polarization analysis of three-component array data, *Bull. Seism. Soc. Am.*, **78**, 1725–1743.

Kennett, B.L.N., 1983. *Seismic Wave Propagation in Stratified Media*, Cambridge University Press, Cambridge.

Kennett, B.L.N., Engdahl, E.R., 1991. Traveltimes for global earthquakes location and phase identification, *Geophys. J. Int.*, **105**, 429–465.

Kind, R., Kosarev, G.L., Petersen, N.V., 1995. Receiver functions at the stations of the German Regional Seismic Network (GRSN), *Geophys. J. Int.*, **121**, 191–202.

Kłaczkowska, M., 2006. Modelowanie pól potencjalnych dla intruzji kętrzyńskiej, *Master's thesis*, University of Warsaw, Warsaw.

Kosarev, G., Kind, R., Sobolev, S.V., Yuan, X., Hanka, W., Oreshin, S., 1999. Seismic Evidence for a Detached Indian Lithospheric Mantle Beneath Tibet, *Science*, **283**, 1306–1309.

Langston, C.A., 1977b. The effect of planar dipping structure on source and receiver responses for constant ray parameter, *Bull. seism. Soc. Am.*, **67**, 1029–1050.

Langston, C.A., 1977a. Corvallis, Oregon, crustal and upper mantle structure from teleseismic P and S waves, *Bull. Seism. Soc. Am.*, **67**, 713–724.

Legendre, C.P., Meier, T., Lebedev, S., Friederich, W., Viereck-Götte, L., 2012. A shear wave velocity model of the European upper mantle from automated inversion of seismic shear and surface waveforms, *Geophys. J. Int*, **191**, 282–304.

Lenardic, A., Moresi, L.N., Jellinek, A.M., Manga, M., 2005. Continental insulation, mantle cooling, and the surface area of oceans and continents, *Earth Planet. Sci. Lett.*, **234**, 317–333.

Levshin A.L., Schweitzer, J., Weidle, C., Shapiro, N.M., Ritzwoller, M.H., 2007. Surface wave tomography of the Barents Sea and surrounding regions, *Geophys. J. Int.*, **170**, 441–459.

Meissner R., 1986. *The continental crust – a geophysical approach*, International Geophysics Series, Academic Press Inc., Orlando, 34, 426 pp.

Polkowski, M., 2012. Local seismic events in area of Trans European Suture Zone based on data from PASSEQ experiment, *Master's thesis*, University of Warsaw, Warsaw.

Polkowski, M., Plesiewicz, B., Wiszniowski, J., Wilde-Piórko, M., PASSEQ Working Group, 2016. Local seismic events in the area of Poland based on data from the PASSEQ 2006-2008 experiment, *Acta Geophysica*, **64**, 2677–2716.

Poppeliers C., Pavlis G.L., 2003. Three-dimensional, prestack, plane wave migration of teleseismic P-to-S converted phases: 1. Theory, *J. Geophys. Res.*, **108**, B2112.

Sambridge, M., 1999a. Geophysical inversion with a neighbourhood algorithm – I. Searching a parameter space, *Geophys. J. Int.*, **138**, 479–494.

Sambridge, M., 1999b. Geophysical inversion with a neighbourhood algorithm – II. Appraising the ensemble, *Geophys. J. Int.*, **138**, 727–746.

Saul, J., Kumar, M.R., Sarkar, D., 2000. Lithospheric and upper mantle structure of the Indian Shield, from teleseismic receiver functions, *Geophys. Res. Lett.*, **27**, 2357–2360.

Trojanowski, J., 2007. Metody Monte Carlo w inwersji funkcji odbioru. *Master's thesis*, University of Warsaw, Warsaw.

Vinnik, L.P., 1977. Detection of waves converted from P to SV in the mantle. *Phys. Earth Planet. Inter.*, **15**, 39–45.

Wachnicka, A., 2005. Struktura skorupy i górnego płaszcza Antarktydy Wschodniej w rejonie stacji Neumayer na podstawie funkcji odbioru, *Master's thesis*, University of Warsaw, Warsaw.

Wilde-Piórko, M., 1997. Sejsmiczna struktura skorupy ziemskiej na podstawie funkcji odbioru stacji Suwałki, *Master's thesis*, University of Warsaw, Warsaw.

Wilde-Piórko, M., 2002a. Modelling of seismic structure of the crust and upper mantle from receiver function, *PhD's thesis*, University of Warsaw, Warsaw.

Wilde-Piórko, M., Chrapkiewicz, K., Lepore, S., Polkowski M., Grad, M., 2016. Complex Modeling of the Seismic Structure of the Trans-European Suture Zone's Margin from Receiver Function Analysis, American Geophysical Union Fall Meeting 2016, San Francisco, 12–16 December 2016, S43B-2891.

Wilde-Piórko, M., Duda, S.J., Grad, M., 2011a. Tomography of Seismic P-Waves from Earthquakes and Explosions — Part II: Morphology of Faulting of the 2004 Sumatra-Andaman Earthquake from Spectral Seismograms, *CT Theory and Applications*, **20**, 465–483.

Wilde-Piórko, M., Duda, S.J., Grad, M., 2011b. Frequency analysis of the 2004 Sumatra-Andaman earthquake using spectral seismograms, *Acta Geophysica*, **59**, 483–501.

Wilde-Piórko M., Geissler W.H., Plomerová J., Grad M., Babuška V., Brückl E., Cyziene J., Czuba W., England R., Gaczyński E., Gazdova R., Gregersen S., Guterch A., Hanka W., Hegedűs E., Heuer B., Jedlička P., Lazauskiene J., Keller G.R., Kind R., Klinge K., Kolinsky P., Komminaho K., Kozlovskaya E., Krüger F., Larsen T., Majdański M., Malek J., Motuza G., Novotný O., Pietrasiak R., Plenefisch T., Růžek B., Sliaupa S., Środa P., Świeczak M., Tiira T., Voss P., Wiejacz P., 2008. PASSEQ 2006-2008: Passive Seismic Experiment in Trans-European Suture Zone, *Stud. Geophys. Geod.*, **52**, 439–448.

Wilde-Piórko, M., Grad, M., POLONIASE Working Group, 1999. Regional and teleseismic events recorded across the TESZ during POLONAISE'97, *Tectonophysics*, **314**, 161–174.

Wilde-Piórko, M., Grad, M., TOR Working Group, 2002b. Differences of the crustal structure between the Precambrian and Palaeozoic platforms in Europe from the inversion of teleseismic receiver function - project TOR, *Geophys. J. Int.*, **150**, 261–270.

Wilde-Piórko M., Grad M., Wiejacz P., Schweitzer J., 2009. HSPB seismic broadband station in Southern Spitsbergen: First results on crustal and mantle structure from receiver functions and SKS splitting, *Pol. Pol. Res.*, **30**, 301-–316.

Zhu, L., Kanamori, H., 2000. Moho depth variation in southern California from teleseismic receiver functions. *J. Geophys. Res.*, **105**, 2969-–2980.

M. Wilde-Piórko